On the Squareness Factor Behavior of RE-FeB (RE = Nd or Pr) Magnets Above Room Temperature

E. A. Périgo[1], H. Takiishi[1], C. C. Motta[2], and R. N. Faria[1]

[1]Nuclear and Energy Research Institute, 05508-000 São Paulo, SP, Brazil
[2]University of São Paulo, 05508-000 São Paulo, SP, Brazil

The magnetic stability of RE-FeB (RE = Nd or Pr) sintered magnets above room temperature was investigated by monitoring the squareness factor (SF). At $293 \leq T \leq 423$ K, commercial anisotropic NdFeB-based sintered magnets with a Curie temperature (T_c) of around 585 K showed no appreciable change in their squareness factors. This indicates that the SF is controlled mainly by the samples' microstructural features. Magnets with $T_c > 593$ K showed a tendency for improved squareness factor at higher temperatures due to the methodology employed to characterize the SF. On the other hand, PrFeCoBCuNb sintered magnets with $T_c > 593$ K presented a reduction in the SF with temperature rising from 298 to 373 K.

***Index Terms*—NdFeB, PrFeB, sintered magnets, squareness factor.**

I. Introduction

In a wide range of technological applications which include motors, acoustics, actuators, and communications, RE-FeB (RE = Nd or Pr) sintered magnets have become key components [1]–[4]. In some of these applications, magnets are exposed to environments above room temperature (T_r). Therefore, the knowledge about the effects of temperature (T) on their magnetic properties is essential for the development of new applications or even for the improvement of existing ones. The increase of T reduces the saturation polarization (J_s) and the magnetocrystalline anisotropy field ($\mu_0 H_a$) of the $Nd_2Fe_{14}B$ compound [5]–[7], leading to a corresponding reduction in the remanence (J_r) and intrinsic coercivity ($\mu_{0J} H_c$) of the magnets. These losses are calculated by the temperature coefficients α and β for J_r and $\mu_{0J} H_c$, respectively. It has been reported that, in the 300–400-K range, $-0.1 \leq \alpha \leq -0.2$%/K and $-0.4 \leq \beta \leq -0.7$%/K [7].

The magnetic stability of a magnet at any temperature can be quantified by its squareness factor (SF). A common way to express it is as follows:

$$\mathrm{SF} = \frac{\mu_0 H_k}{\mu_{0J} H_c} \tag{1}$$

where $\mu_0 H_k$ is the knee field corresponding to a magnetization of 90% of J_r [8]. Another method to determine the squareness of the $J \times \mu_0 H$ curve in the second quadrant is the ratio of the area below the demagnetization curve to the product of J_r and $\mu_{0J} H_c$, called rectangularity [9]. A discussion is also given in [10].

From (1), it could be expected that SF = SF(T) due to the dependence of both $\mu_0 H_k$ and $\mu_{0J} H_c$, in distinct magnitudes, on temperature. On the other hand, it has been suggested that the squareness factor of anisotropic $Nd_{16}Fe_{76}B_8$ and $Pr_{16}Fe_{76}B_8$ sintered magnets would be controlled mainly by their microstructural features, according to the expression [11]

$$\mathrm{sf} = 1 - \left[\frac{\sigma_{GS}}{\bar{\times}_{GS}} \left(\frac{\sigma_E}{\bar{\times}_E} + \frac{\sigma_R}{\bar{\times}_R} \right) \right] \tag{2}$$

where $\bar{\times}_{GS}$, $\bar{\times}_E$, and $\bar{\times}_R$ are the mean size, mean elongation, and mean roundness of the hard magnetic grains and σ_{GS}, σ_E, and σ_R are their respective standard deviations. Expression (2) does not describe any dependence of the squareness factor on T. Therefore, in order to clarify this point, the effect of temperature on the magnetic stability of RE-FeB-based sintered magnets was investigated here by monitoring the SF.

II. Data Acquisition

Table I lists the features of the NdFeB-based sintered magnets considered in this work. Six commercial grades were selected from three magnet suppliers [12]–[14] and were grouped according to their maximum energy products $[(BH)_{\max}]$ and Curie temperatures (T_c). Based on (1), the squareness factors were calculated from the demagnetization curves available online for $293 \leq T \leq 423$ K. The data were normalized by the ratio of the squareness factor for each available temperature above 293 K to the squareness factor at room temperature, identified hereinafter as $\mathrm{SF_{norm}}$. For the classification of each magnet (type A, B, etc.), a mean value of $\mathrm{SF_{norm}}(\mathrm{SF_{norm}})$ and its respective standard deviation σ_{SF} were determined, based on at least five distinct temperatures.

For comparison, PrFeB sintered magnets were prepared according to [15]. The samples with alloying elements were obtained by the alloy mixing technique. The SF was also determined using (1), based on the demagnetization curves for $T =$ 298 K and $T = 373$ K. Remanence and intrinsic coercivity temperature coefficients for these magnets were found based on the methodology reported on [16]. Albeit typical for NdFeB magnets, the second quadrant of PrFeB magnets above room temperature is not often showed and/or discussed. All the PrFeB samples presented a mean grain size of about 4 μm.

Manuscript received March 03, 2009. Current version published September 18, 2009. Corresponding author: E. A. Périgo (e-mail: eaperigo@ieee.org).
Digital Object Identifier 10.1109/TMAG.2009.2025190

TABLE I
IDENTIFICATION, MAXIMUM ENERGY PRODUCT, CURIE TEMPERATURE, AND COEFFICIENTS α AND β OF THE COMMERCIAL NDFEB SINTERED MAGNETS CONSIDERED IN THIS WORK [12]–[14]

Type	$(BH)_{max}$ (kJm^{-3})	T_c (K)	α (% / K)	β (% / K)
A	309 – 333	583	- 0.12	-0.60 – -0.63
B	349 – 374	583	-0.12	-0.60 – -0.63
C	374 – 398	583 – 593	-0.12	-0.60 – -0.61
D	252 – 276	603 – 633	-0.11	-0.55 – -0.58
E	268 – 293	603 – 633	-0.11	-0.55 – -0.58
F	309 – 333	603 – 633	-0.11	-0.55 – -0.58

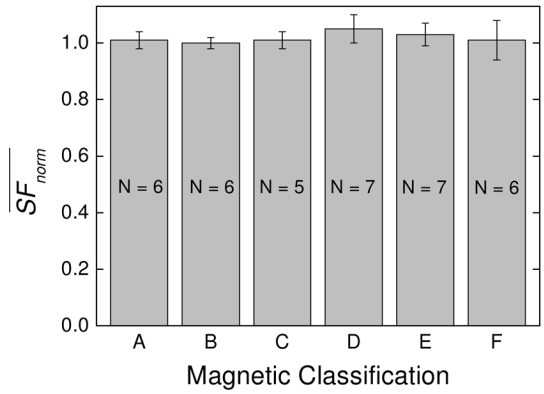

Fig. 1. Mean normalized squareness factor and respective standard deviations of the commercial anisotropic NdFeB sintered magnets considered in this work. The number inside each column refers to the amount of temperatures considered to determine SF_{norm} and σ_{SF}.

III. RESULTS AND DISCUSSION

Fig. 1 shows the mean normalized squareness factor and the standard deviation of the commercial anisotropic NdFeB sintered magnets for $293 \leq T \leq 423$ K. Type A, B, and C magnets showed almost unchanged SF_{norm}, close to unity, and their respective σ_{SF} showed a maximum value of 0.03. Therefore, the squareness factor in the temperature range evaluated here showed a value very similar to that obtained at T_r. For type D, E, and F magnets, the temperature rising caused a slight increase of SF_{norm} and/or σ_{SF}. It could be expected since, based on the coefficients α and β, the intrinsic coercivity declines more rapidly than the remanence by a factor of approximately 5 (see Table I). Intrinsic coercivity is contained in the denominator of (1), so the squareness factor should be higher at higher temperatures, thus increasing SF_{norm}. These reported SF versus T behaviors take into account that the squareness factor is expressed by (1). Therefore, a change in the methodology to establish SF could also modify the results, although the shape of the demagnetization curves of the sintered magnets evaluated here are quite similar within the temperature range investigated. The tendency for improvement of the squareness factor with rising temperatures has been identified in magnets with $T_c > 593$ K, which is influenced by the chemical composition of the magnetic alloy. Such behaviors (constancy and/or slight improvement of SF) can be verified in [16] and [17].

The behavior of the squareness factor above room temperature for commercial anisotropic NdFeB sintered magnets is in satisfactory agreement with (2). Therefore, it is reasonable to assume that no microstructural changes occurred during the magnetic characterizations reported here. To confirm this assumption, an evaluation was made of the phase transformations, densification, and grain size and/or shape modification in NdFeB-based alloys.

Starting from room temperature, the first reaction takes place at 928 K [18], [19], which is the melting of the rare earth-rich phase. This temperature is approximately 2.2-fold higher than the maximum temperature employed in magnetic characterizations by magnet suppliers (423 K). This liquid phase must be considered because the hard magnetic grains have to be enclosed by it in order to develop a high $\mu_0 J H_c$, which will certainly influence SF according to (1). Moreover, the temperature of this reaction also depends on the chemical composition of the magnetic alloy. Some elements such as copper can lower it to 758 K [20], which is still 1.8-fold higher than the maximum magnetic characterization temperature. In addition, melting of the rare earth-rich phase marks the beginning of densification of NdFeB magnets [19] and this event also did not occur.

Depending on their chemical composition and cooling rate during fabrication, NdFeB-based alloys may also present secondary phases that can be detrimental to the intrinsic coercivity and/or to the squareness factor. Examples are Fe-α and η ($Nd_{1+\varepsilon}Fe_4B_4$). Fe-$\alpha$ is a reverse domain nucleation center in RE-FeB sintered magnets, reducing $\mu_0 J H_c$ and SF. To avoid it, a heat treatment is required. For an $Nd_{13.33}Fe_{80.00}B_{6.67}$ (% at.) alloy, it was found that the minimum time necessary to eliminate Fe-α was 1.6 h at 1358 K [21]. Once again, this annealing temperature is far above (3.2-fold) that of the maximum magnetic characterization temperature. As for the η phase, it was observed that large volumes at grain boundaries may be deleterious to SF [11] and a homogeneous distribution of it is desirable in order to diminish its influence on SF. Furthermore, $Nd_{1+\varepsilon}Fe_4B_4$ reportedly has a Curie temperature near 50 K [22]. Hence, it is also possible that it contributes to the large step in the demagnetization curve at 4.2 K, together with the spin reorientation of the Nd_2Fe_{14} B compound, which is deleterious to the squareness factor of a magnet even in the absence of microstructural changes.

Milling, sintering and postsintering annealing are the key processes which directly affect grain size and/or shape in RE-FeB sintered magnets, and can therefore modify the squareness factor. The effects of milling on RE-FeB sintered magnets have already been investigated. In general, long milling times are necessary to obtain high magnetic properties and SF [23] because of microstructural homogenization, as stated in (2). With regard to sintering, the heating of a green body up to the shrinkage temperature will cause the growth and the modification of the shape of hard magnetic particles. Sintering is usually carried out above 1273 K to reduce porosity to a minimum level [24]–[27] in order to obtain high remanence (since J_r is proportional to the packing factor of the magnet) and intrinsic coercivity (pores may act as reverse domain nucleation centers). This value is approximately threefold that of the maximum temperature used in magnetic characterizations. Postsintering annealing to enhance $\mu_0 J H_c$ has also been investigated and several works report that this step is carried out at no less than

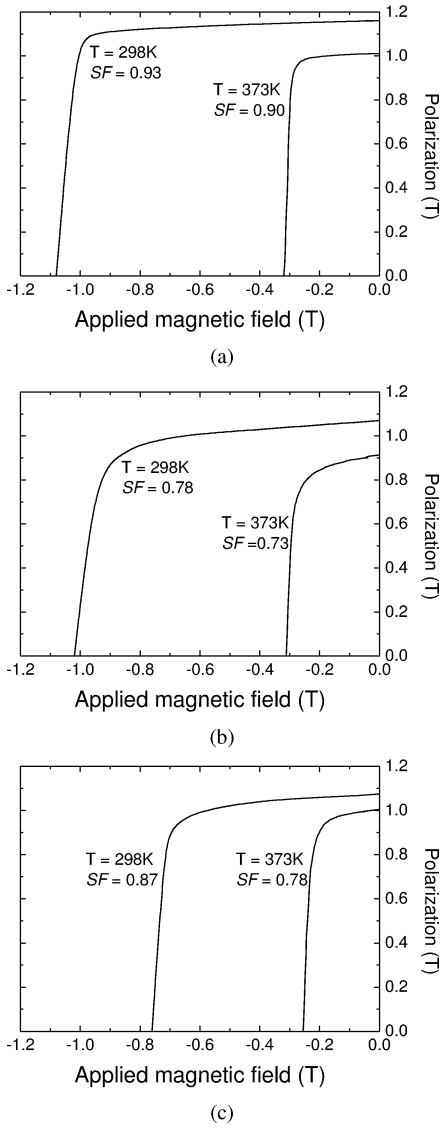

Fig. 2. Demagnetization curves of sintered magnets prepared in this work. (a) $Pr_{16}Fe_{76}B_8$. (b) $Pr_{15.30}Fe_{bal}Co_{3.20}B_{5.80}Cu_{0.40}Nb_{0.08}$. (c) $Pr_{16.60}Fe_{bal}Co_{9.60}B_{5.60}Cu_{0.80}Nb_{0.06}$.

673 K [28]–[30]. Furthermore, this heat treatment must not be extended for long periods of time in order to prevent the intrinsic coercivity from diminishing due to excessive grain growth and deterioration of SF attributed to inhomogeneous grain distribution [31] which, again, is in agreement with (2).

PrFeB sintered magnets should also show a behavior similar to that of the squareness factor as a function of temperature variations comparable to that discussed for NdFeB sintered magnets. This is expected because the PrFeB ternary system presents correspondences with the NdFeB ternary system. A comparison of the microstructure of PrFeB and NdFeB samples indicated they were similar in the as-cast state and after annealing at 873 K [32]. However, PrFeB sintered magnets are less susceptible to microstructural changes than NdFeB sintered magnets are to sintering and postsintering annealing due to a slower kinetics [19], [32]. Moreover, the $Pr_2Fe_{14}B$ compound shows no spin reorientation below T_r.

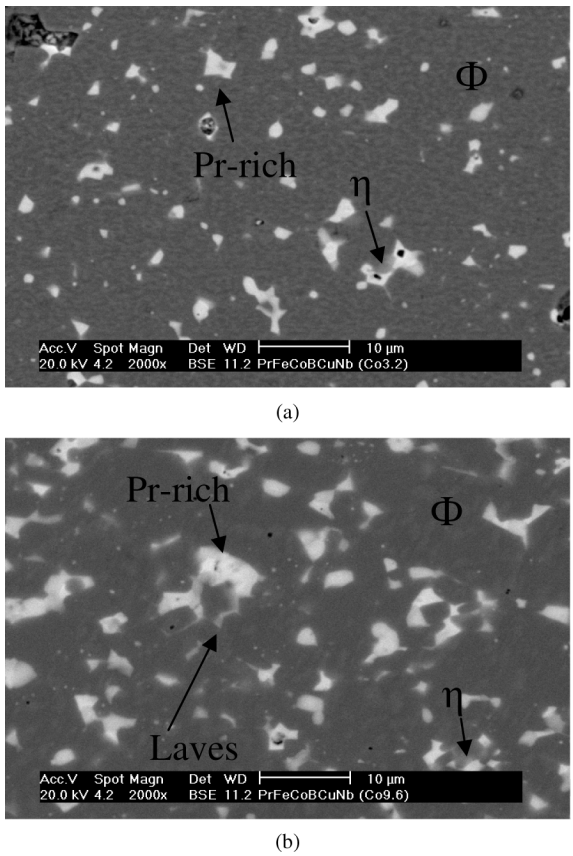

Fig. 3. Backscattered electron image of (a) $Pr_{15.30}Fe_{bal}Co_{3.20}B_{5.80}Cu_{0.40}Nb_{0.08}$ magnet, and (b) $Pr_{16.60}Fe_{bal}Co_{9.60}B_{5.60}Cu_{0.80}Nb_{0.06}$ magnet. The phases are indicated.

For the $Pr_{16}Fe_{76}B_8$ composition ($T_c = 565$ K [7]), the SF value for $T = 373$ K was slightly lower than that verified at T_r, as depicted in Fig. 2(a). This discrepancy was considered within the experimental error and consistent with (2), since no microstructural modifications were expected. Remanence and intrinsic coercivity temperature coefficients are, respectively, -0.16%/K and -0.88%/K. The former is within the range reported in [7] for NdFeB sintered magnets and the latter is larger than the superior limit value (-0.7%/K). On the other hand, sintered magnets containing alloying elements (niobium, copper, and mainly cobalt) showed more pronounced changes in SF. The $Pr_{15.30}Fe_{bal}Co_{3.20}B_{5.80}Cu_{0.40}Nb_{0.08}$ composition revealed a reduction of the squareness factor (from 0.78 to 0.73) in a comparison of the $J \times \mu_0 H$ curves at $T = 298$ K and $T = 373$ K, showed in Fig. 2(b), and a more pronounced decrease of SF was verified in another composition richer in Co [$Pr_{16.60}Fe_{bal}Co_{9.60}B_{5.60}Cu_{0.80}Nb_{0.06}$; see Fig. 2(c)]. This behavior is the opposite of that previously reported for commercial NdFeB-based sintered magnets (it is worth pointing out that both magnets present $T_c > 565$ K). The increasing of cobalt on magnets composition also reduced α in a larger magnitude compared to β, where the latter remains comparable to that observed in the $Pr_{16}Fe_{76}B_8$ magnet. Therefore, the addition of Co to PrFeB sintered magnets causes two effects: 1) it is beneficial to the Curie temperature $\mu_0 H_a$ (starting from

a given Co concentration for the latter) [33], α, and β; and 2) deleterious to J_s [33] and apparently to SF.

Microstructures of the magnets with compositions containing cobalt, niobium, and copper are showed in Fig. 3(a) and (b). An analysis of the existing phases in these samples indicated that the $Pr_{15.30}Fe_{bal}Co_{3.20}B_{5.80}Cu_{0.40}Nb_{0.08}$ magnet has basically three phases: $Pr_2(Fe,Co)_{14}B$, Pr-rich, and η phase. With regards to the $Pr_{16.60}Fe_{bal}Co_{9.60}B_{5.60}Cu_{0.80}Nb_{0.06}$ magnet, a fourth phase was found (Laves). Finally, it is worth pointing out that the discrepancy in the squareness factor at $T > T_r$ for PrFeB-based sintered magnets was observed in the samples containing cobalt, whose Curie temperature increased, similar to what occurred in NdFeB sintered magnets. An investigation on this subject is already in progress.

ACKNOWLEDGMENT

This work was supported by the Nuclear and Energy Research Institute (IPEN-CNEN) and the Fundação de Amparo à Pesquisa do Estado de São Paulo (FAPESP) under Contract 2005/04711-2. The authors would like to thank E. A. Ferreira, P. A. P. Wendhausen, and L. U. Lopes.

REFERENCES

[1] K. Yamazaki, M. Shina, M. Miwa, and J. Hagiwara, "Investigation of eddy current loss in divided Nd-Fe-B sintered magnets for synchronous motors due to insulation resistance and frequency," *IEEE Trans. Magn.*, vol. 44, no. 11, pp. 4269–4272, Nov. 2008.

[2] S. Ruoho and A. Arkki, "Partial demagnetization of permanent magnets in electrical machines caused by an inclined field," *IEEE Trans. Magn.*, vol. 44, no. 7, pp. 1773–1778, Jul. 2008.

[3] H. Saotome, T. Okubo, and Y. Ikeda, "Novel actuator with Nd-Fe-B magnets swimming in parallel to the magnetic field," *IEEE Trans. Magn.*, vol. 38, no. 5, pp. 3009–3011, Sep. 2002.

[4] Y. Matsuura, "Recent development of Nd-Fe-B sintered magnets and their applications," *J. Magn. Magn. Mater.*, vol. 303, no. 2, pp. 344–347, 2006.

[5] K.-D. Durst and H. Kronmüller, "Determination of intrinsic magnetic material parameters of $Nd_2Fe_{14}B$ from magnetic measurements of sintered $Nd_{15}Fe_{77}B_8$ magnets," *J. Magn. Magn. Mater.*, vol. 59, no. 1–2, pp. 86–94, 1986.

[6] A. Fukuno, K. Hirose, and T. Yoneyama, "Coercivity mechanism of sintered NdFeB magnets having high coercivities," *J. Appl. Phys.*, vol. 67, no. 9, pp. 4750–4752, 1990.

[7] J. F. Herbst, "$R_2Fe_{14}B$ materials: Intrinsic properties and technological aspects," *Rev. Mod. Phys.*, vol. 63, no. 4, pp. 819–898, 1991.

[8] D. J. Branagan, M. J. Kramer, Y. L. Tang, and R. W. McCallum, "Maximizing loop squareness by minimizing gradients in the microstructure," *J. Appl. Phys.*, vol. 85, no. 8, pp. 5923–5925, 1999.

[9] H. Zhang, S. Zhang, B. Shen, and H. Kronmüller, "Magnetization behavior of nanocrystalline permanent magnets based on the Stoner-Wohlfarth model," *J. Magn. Magn. Mater.*, vol. 260, pp. 352–360, 2003.

[10] , É. T. de Lacheisserie, D. Gignoux, and M. Schlenker, Eds., *Magnetism: Materials and Applications*. New York: Springer-Verlag, 2005, p. 12.

[11] E. A. Périgo, H. Takiishi, C. C. Motta, and R. N. Faria, "Microstructure and squareness factor: A quantitative correlation in (Nd, Pr)FeB sintered magnets," *J. Appl. Phys.*, vol. 102, p. 113912, 2007.

[12] MMC Corporation, accessed: July 2 2008 [Online]. Available: http://www.mmcmagnetics.com/ourproducts/main_NdFeB.htm#sintered

[13] Xinchang Magnet Industry Co. Ltd., accessed: July 2 2008 [Online]. Available: http://www.magnet-product.com/demag_curves.htm

[14] Dexter Magnetic Technologies, accessed: July 2 2008 [Online]. Available: http://www.dextermag.com/Neodymium-Iron-Boron.aspx

[15] E. P. Soares, E. A. Périgo, H. Takiishi, C. C. Motta, and R. N. Faria, "A study of PrFeB magnets produced by a low-cost powder method and the hydrogen decrepitation process," *Mater. Res.*, vol. 8, pp. 143–145, 2005.

[16] B. M. Ma and K. S. V. L. Narasimhan, "Temperature dependence of magnetic properties of Nd-Fe-B magnets," *J. Magn. Magn. Mater.*, vol. 54–47, pp. 559–562, 1986.

[17] D. Li, H. F. Mildrum, and K. J. Strnat, "Permanent magnet properties of sintered Nd-Fe-B between -40 and $+200°$C," *J. App. Phys.*, vol. 57, no. 1, pp. 4140–4142, 1985.

[18] G. Schneider, F. J. G. Landgraf, and F. P. Missel, "Additional ferromagnetic phases in the Fe-Nd-B system and the effect of a 600°C annealing," *J. Less-Common Met.*, vol. 153, no. 1, pp. 169–180, 1989.

[19] M. G. Taylor, B. E. Davies, and I. R. Harris, "A comparative study of the sintering behavior of NdFeB and PrFeB for permanent magnet applications," *J. Magn. Magn. Mater.*, vol. 242–245, no. 2, pp. 1375–1377, 2002.

[20] , J. M. D. Coey, Ed., *Rare Earth Iron Permanent Magnets*. Oxford, U.K.: Clarendon Press, 1996, p. 168.

[21] W. C. Chang, T. S. Chin, and K. S. Liu, "The dissolution kinetics of free iron in Nd-Fe-B permanent magnet alloys," *J. Magn. Magn. Mater.*, vol. 80, no. 2–3, pp. 352–358, 1989.

[22] K. Kuntze, D. Kohake, R. Beranek, S. Stieler, and C. Heiden, "Temperature dependence of magnetization reversal of sintered Nd-Fe-B magnets," *J. Phys.*, vol. 46-C6, no. 9, pp. C6-253–C6-257, 1985.

[23] A. Kianvash and I. R. Harris, "The production of a $Nd_{16}Fe_{76}B_8$ sintered magnet by the hydrogen decrepitation/hydrogen vibration milling route," *J. Alloys Comp.*, vol. 282, no. 1–2, pp. 213–219, 1999.

[24] R. S. Mottram, A. J. Williams, and I. R. Harris, "The effects of blending additions of copper and cobalt to $Nd_{16}Fe_{76}B_8$ milled powder to produce sintered magnets," *J. Magn. Magn. Mater.*, vol. 234, no. 1, pp. 80–89, 2001.

[25] A. M. Gabay, Y. Zhang, and G. C. Hadjipanayis, "Effect of very small additions on the coercivity of Dy-free Nd-Fe-(Co)-B-sintered magnets," *J. Magn. Magn. Mater.*, vol. 238, no. 2–3, pp. 226–232, 2002.

[26] H. R. M. Hosseini and A. Kianvash, "The role of milling atmosphere on microstructure and magnetic properties of a $Nd_{12.8}Fe_{79.8}B_{7.4}$-type sintered magnet," *J. Magn. Magn. Mater.*, vol. 281, no. 1, pp. 92–96, 2004.

[27] M. Yan, L. Q. Yu, W. Luo, W. Wang, W. Y. Zhang, and Y. H. Wen, "Change of microstructure and magnetic properties of sintered Nd-Fe-B induced by annealing," *J. Magn. Magn. Mater.*, vol. 301, no. 1, pp. 1–5, 2006.

[28] V. P. Menushenkov and A. G. Savchenko, "Effects of post-sintering annealing on magnetic properties of Nd-Fe-B sintered magnets," *J. Magn. Magn. Mater.*, vol. 258–259, pp. 558–560, 2003.

[29] H. Kato, T. Miyazaki, M. Sagawa, and K. Koyama, "Coercivity enhancements by high-magnetic-field annealing in sintered Nd-Fe-B magnets," *Appl. Phys. Lett.*, vol. 84, no. 21, pp. 4230–4232, 2004.

[30] H. Wang, A. Li, Y. Guo, M. Zhu, and W. Li, "The effect of element doping and heat treatment on the impact resistance of Nd-Fe-B sintered magnets," *J. Appl. Phys.*, vol. 103, 2008, 07E119.

[31] M. R. Corfield, A. J. Williams, and I. R. Harris, "The effects of long term annealing at 1000°C for 24 h on the microstructure and magnetic properties of Pr-Fe-B/Nd-Fe-B magnets based on $Nd_{16}Fe_{76}B_8$ and $Pr_{16}Fe_{76}B_8$," *J. Alloys Comp.*, vol. 296, no. 1–2, pp. 138–147, 2000.

[32] A. C. Neiva, A. P. Tschiptschin, and F. P. Missel, "Phase diagram of the Pr-Fe-B system," *J. Alloys Comp.*, vol. 217, no. 2, pp. 273–282, 1995.

[33] A. T. Pedziwiatr, S. Y. Jiang, and W. E. Wallace, "Structure and magnetism of the $Pr_2Fe_{14-x}Co_xB$ system," *J. Magn. Magn. Mater.*, vol. 62, no. 1, pp. 29–35, 1986.